

Final Draft
of the original manuscript:

Enz, J.; Kumar, M.; Riekehr, S.; Venzke, V.; Huber, N.; Kashaev, N.:
**Mechanical properties of laser beam welded similar and
dissimilar aluminum alloys**

In: Journal of Manufacturing Processes (2017) Elsevier

DOI: 10.1016/j.jmapro.2017.07.030

Mechanical properties of laser beam welded similar and dissimilar aluminum alloys

Authors: J. Enz^{1,2}, M. Kumar³, S. Riekehr¹, V. Ventzke¹, N. Huber¹, N. Kashaev¹

Affiliations:

¹Helmholtz-Zentrum Geesthacht, Institute of Materials Research, Materials Mechanics, Max-Planck-Straße 1, 21052 Geesthacht, Germany;

²TuTech Innovation GmbH, Harburger Schloßstraße 6-12, 21079 Hamburg, Germany;

³Light Metals Technologies Ranshofen, Austrian Institute of Technology, 5282 Ranshofen, Austria.

Corresponding author: J. Enz, Tel.: +49-4152-87-2507, Fax: +49-4152-87-42507,
E-mail: josephin.enz@hzg.de

Abstract:

Two approaches were used for laser beam welding of similar and dissimilar joints of AA7075 and AA5182 that aim to overcome the weldability problems of high-strength Al-Zn-Mg-Cu alloys. The first approach implies the use of vanadium foil as additional filler material, while the second implies the use of a fiber laser with a large beam diameter and a top-hat beam profile. Although both approaches result in an improved weld quality, in terms of weld appearance, porosity and cracking, the resulting mechanical properties differ considerably. The addition of vanadium leads to a local increase of microhardness in the fusion zone. However, the tensile strength of these joints is lower as for fiber laser welded joints. In direct comparison fiber laser welded joints exhibit also higher formability as the joints welded with vanadium foil. The highest formability is obtained for dissimilar joints with the medium-strength Al-Mg alloy. Due to the unavoidable softening in the weld zone of heat treatable aluminum alloys, the formability of the joints is inferior in comparison to the base materials. In

addition, the positive effect of post-weld heat treatment, surface milling and warm forming on the resulting mechanical properties of similar and dissimilar joints is discussed.

Keywords: Al-Zn-Mg-Cu alloy; Al-Mg alloy; laser beam welding; dissimilar joint; mechanical property; sheet metal forming.

1. Introduction

High-alloyed Al-Zn-Mg-Cu alloys, with a (Zn+Mg+Cu) content above 10 wt.%, are generally assumed to be non-weldable by fusion welding techniques, such as laser beam welding (LBW) [1]. The laser weldability problems are characterized by an inferior outer appearance of the weld, mainly due to the expulsion of weld metal during laser beam welding, and by high porosity as well as severe cracking [2,3]. Solely by solid state welding, such as friction stir welding, defect-free weld seams can be achieved [4]. However, solid state welding is often not common or even not applicable for high-capacity industrial productions, due to its difficulties to weld complex structures and to control tolerances [5,6]. Because of their high strength in combination with a low density, Al-Zn-Mg-Cu alloys are promising materials for light-weight structures in the automotive industry, especially in comparison to steels (Fig. 1). Since laser beam welding is already established in the automotive industry as an efficient joining technology for series production, the laser weldability and adequate resulting mechanical properties have to be proved before the implementation of a new material to production. Al-Mg and Al-Mg-Si alloys exhibit acceptable laser weldability and a good formability. For this reason, these medium-strength aluminum alloys are predominantly used in the automotive industry for the substitution of steel, whereas high-strength Al-Zn-Mg-Cu alloys are currently unrecognized [7,8].

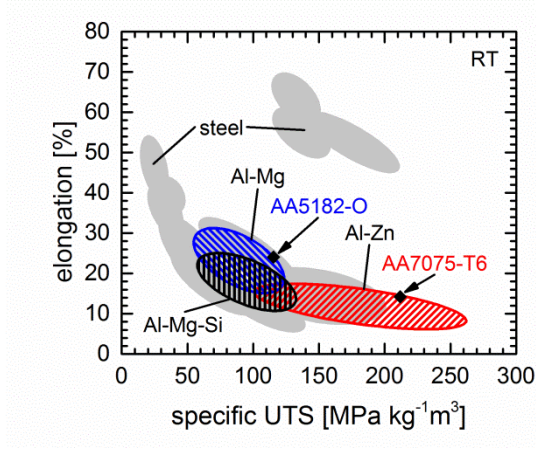


Fig. 1: Elongation and specific ultimate tensile strength of different aluminum alloys for the automotive industry in comparison to steels (according to van Nieuwerburgh [8]).

Besides light-weighting, the tailoring of structural properties is of great importance for the automotive industry. In this regard, the laser beam welding of dissimilar joints, so-called tailor-welded blanks (TWB), becomes necessary. The sheets can differ in their thickness, temper condition as well as in their chemical composition, so that locally different mechanical properties of the welded structure result [9]. A secondary effect of this tailoring is the saving of structural weight. However, due to changed chemical composition of the melt, the weldability of dissimilar joints may also alter. For this reason, most often similar weldable aluminum alloys with differing sheet thicknesses or temper conditions are preferred for fusion welding [10-13,15,16]. In case of friction stir welding, these weldability problems for dissimilar joints were not observed [17]. In contrast to steel, all precipitation-hardenable aluminum alloys exhibit softening in the weld zone, which is increasing with increasing strength for high-strength aluminum alloys [19,20]. This has an influence on the resulting formability of the TWB and represents, besides the weldability, the second challenge to be coped before the implementation of high-alloyed Al-Zn-Mg-Cu alloys.

Recently, two approaches were developed by the authors [21,22] for improving the laser weldability of high-alloyed Al-Zn-Mg-Cu alloys. Therefore, the thermophysical properties of the main constituents of these alloys during laser beam welding were examined and their influence on laser weldability was deduced. It turned out that the use of an adequate filler material can positively influence the thermophysical properties of the melt. Vanadium, for example, increases the surface tension and viscosity of the melt, decreases the beam irradiance and contributes to the balance between keyhole and vapor pressure. By this first approach, the keyhole stability during laser beam welding and thus the weld quality can also be improved [21]. This positive effect on the laser weldability could not be achieved solely by the use of a conventional aluminum alloy filler wire, since the thermophysical properties are only marginally different. Moreover, its effect on the resulting mechanical properties is also very limited [14]. In case of the second approach, the keyhole stability is improved by the use of a high-power fiber laser with an enlarged beam diameter, a top-hat beam profile and a high beam quality. Thus, the beam irradiance is decreased and the pressure balance achieved. And although no additional filler material is used for laser beam welding, the weld quality can be improved too [22]. The effectiveness of both approaches was demonstrated for similar joints even for very high alloyed Al-Zn-Mg-Cu alloy, such as AA7034 [21,22].

In the present study, the characteristics of the Al-Zn-Mg-Cu alloy joints welded with both developed approaches are compared with special regard to the resulting mechanical properties. Besides similar joints of an Al-Zn-Mg-Cu alloy, dissimilar joints with an Al-Mg alloy were laser beam welded in order to examine the capability of the approaches for the manufacturing of TWB's. In this regard, the challenge lies in combining materials exhibiting clearly different weldability and mechanical properties. Moreover, options for improving the mechanical properties of the joints, such as post-

weld heat treatment, surface milling and warm forming, are examined. This allows the assessment of the potential of high-alloyed Al-Zn-Mg-Cu alloys for the use in the automotive industry.

2. Materials and experimental procedure

2.1. Base and filler materials

The precipitation-hardenable Al-Zn-Mg-Cu alloy 7075 was used for the welding of similar joints. For the dissimilar joints, the naturally aged Al-Mg alloy 5182 was used. By this means, a high-strength material was combined with a material of high formability in a tailor-welded blank. The sheet thickness of both alloys was 2 mm. The chemical composition as well as the temper condition of both alloys is given in Table 1.

For the welding of the first approach 99.8% pure vanadium was used additional to a conventional filler material. Therefore, a vanadium foil with thickness of 40 µm was laser tack welded on the face side of one sheet, in order to ensure the position of the foil during welding. Moreover, the commercial Al-Mg filler wire 5087 (Table 1) with a wire diameter of 1.0 mm was fed during welding. In contrast, no specific filler material was required for the second approach.

Table 1: Chemical composition (in wt.%) and temper condition of the used aluminum alloys.

alloy (temper)	Si	Fe	Cu	Mn	Mg	Cr	Zn	Ti	Al
AA7075 (T6)	0.4	0.5	2.0	0.3	2.9	0.28	6.1	0.2	Bal.
AA5182 (O)	0.2	0.35	0.15	0.5	5.0	0.1	0.25	0.1	Bal.
AA5087 (-)	0.25	0.4	0.05	1.1	5.2	0.25	0.25	0.15	Bal.

Prior to welding, the surface of the aluminum sheets was mechanically grinded and cleaned subsequently with alcohol. In this way, the oxide layer as well as surface

contaminations were removed to eliminate a possible source for hydrogen-induced porosity.

2.2. Laser beam welding

The two approaches for improving laser weldability imply the use of two different laser systems. A medium-power Nd:YAG laser – widely used in the industry – with a small beam diameter of approximately 366 µm and a Gaussian beam profile was used for the implementation of the first approach, since no special requirements on the laser system were made. For the second approach a high-power Yb fiber laser with a beam diameter of 746 µm, which is twice as large as of the Nd:YAG laser, and a top-hat beam profile was employed. The characteristics of both laser systems are specified in Table 2.

Table 2: Laser systems and parameters used for welding of the similar and dissimilar joints.

property	1 st approach	2 nd approach
laser type	Nd:YAG	Yb fibre
wavelength	1.064 µm	1.070 µm
beam parameter product	14.528 mm mrad	11.305 mm mrad
fiber diameter	300 µm	300 µm
focal length	250 mm	300 mm
collimator length	200 mm	150 mm
laser spot diameter (in focus)	366 µm	746 µm
Rayleigh length	4.63 mm	24.55 mm
irradiance distribution	Gaussian	top-hat
laser power	2.0 kW	3.0 kW
focus position	0 mm	+7.5 mm
welding speed	3500 mm/min	3500 mm/min
feed rate of filler wire	3000 mm/min	-

flow rate of shielding gas	20 l/min	20 l/min
----------------------------	----------	----------

The laser beam welding process parameters given in Table 2 were optimized for each approach with regard to the weld quality. The defocusing of +7.5 mm in case of the second approach led to a further increase of the beam diameter to 882 µm. In addition, a higher laser power was required, due to the larger interaction area of the laser on the sheet surface. Although different aluminum alloys were used, no adjustment of the welding parameters was required for the dissimilar joint. For both joint configurations, the weld line was oriented longitudinal to the rolling direction of the sheets.

The filler wire for the first approach was fed in the dragging configuration. For both approaches argon was used as shielding gas, which was supplied from top and root side of the weld, in order to avoid hydrogen-induced porosity and oxidation in the weld zone.

2.3. Non-destructive testing

The assessment of the weld quality was carried out by non-destructive testing. Visual testing was performed for assessing the outer appearance of the weld. Inner defects, such as pores and cracks, were detected with the help of radiographic inspection according to EN ISO 17636-1.

2.4. Destructive testing

The characteristics of the resulting joints were determined by metallographic investigation. The local mechanical properties were determined by Vickers microhardness measurement according to DIN EN ISO 6507-1 with a load of 0.2 kp and loading time of 10 s. Post-weld heat treatment (PWHT) to the peak aged temper condition T6 was chosen for assessing the possibility of improving the hardness in the fusion and heat affected zone. Therefore, a solution heat treatment at 470°C for 1

hour followed by quenching in water and artificial ageing at 120°C for 24 hours was done. Flat tensile testing according to ISO 6892-1 as well as limit dome height testing (LDH) was performed in order to determine the global mechanical properties such as formability of the laser welded joints. Two types of surface conditions were used for tensile testing – the as-welded condition and the mechanically milled condition. By this, it was possible to exclude the effect of geometrical discontinuities. The tensile testing speed was 1 mm/min. Forming tests were performed at room temperature (RT) and at elevated temperatures of 230°C for assessing the possibility of improving formability. Therefore, a computer controlled servo-hydraulic press with a 100 mm diameter hemispherical punch and an optical deformation measuring system was used. The punch speed was 90 mm/min. During testing, the blanks with a size of 180 mm x 180 mm were clamped with a force of 300 kN. For the evaluation of the hydrogen influence on the resulting weld quality, the average hydrogen content of the AA7075 base material and of the extracted fusion zones of the similar joints welded of both approaches was determined by using the hot gas extraction method.

3. Results and discussion

3.1. Weld seam quality

The visual testing confirms the positive effect of both approaches on the laser weldability even for the dissimilar joints, as it can be seen in Fig 2. The outer appearance of all welds is very uniform and no outer weld discontinuities are visible, as it was observed for high-alloyed Al-Zn alloys welded with conventional fusion welding techniques [1-3,21,22].

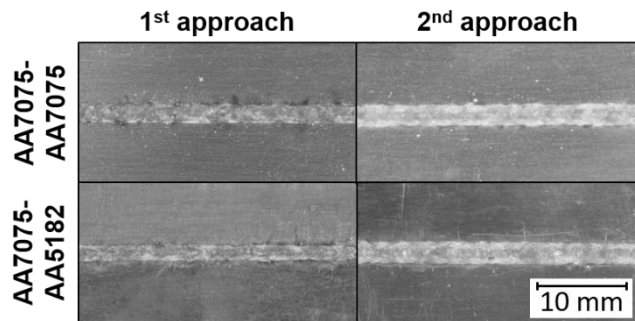


Fig. 2: Effect of the developed approaches on the outer weld seam appearance of the similar AA7075-AA7075 joints.

In Fig. 3a the radiographs of the joints of both approaches are depicted. In case of the joints of the first approach an increase of the material density (resulting in a reduced blackening of the radiographic film) in the fusion zone (FZ) was observed. This can be explained by the addition of high density vanadium (with 6 g/cm^3) to the low density aluminum weld metal (with 2.7 g/cm^3). Furthermore, it can be seen that the vanadium is almost homogeneously distributed in the fusion zone. Here, it has to be mentioned that the vanadium is not entirely dissolved and very small vanadium inclusions are visible. An example for insufficient melting of the vanadium foil is shown in Fig. 3b. This kind of discontinuity occurred only in case of inaccurate positioning of the vanadium foil and laser beam for welding. The joints welded with the fiber laser exhibit a very homogeneous weld seam, since no filler material was added. All joints welded with the approaches do not possess any severe weld inner discontinuity.

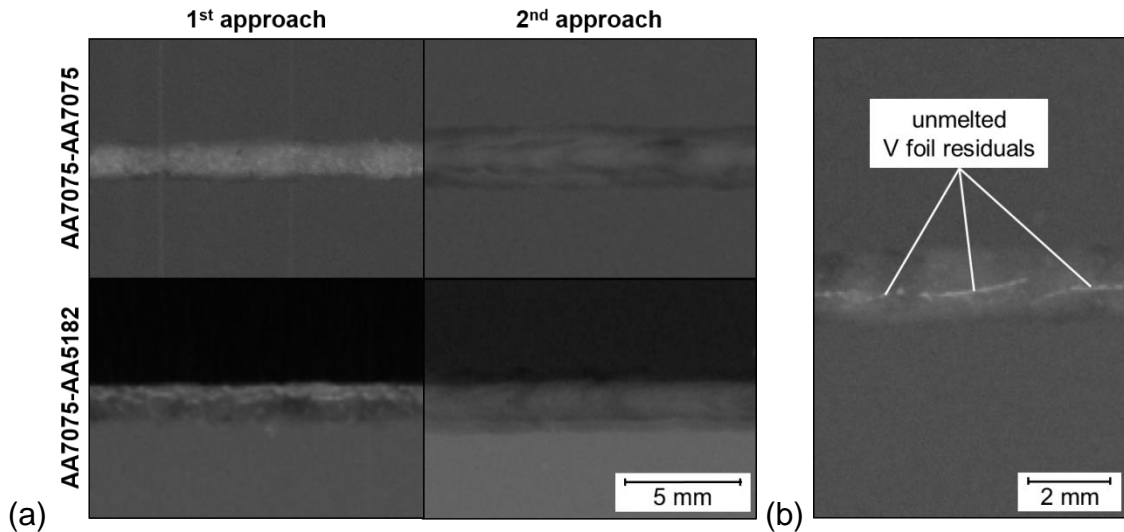


Fig. 3: Radiographs of the similar and dissimilar joints laser beam welded with both approaches (a) and an example for insufficient melting of the vanadium foil (b).

In the macrographs (Fig. 4) the differences of the weld seam size and shape of both approaches are visible. The reason for this is the use of different laser welding parameters and beam diameters. Furthermore, the joints of the first approach exhibit undissolved vanadium foil residuals, which could hardly be avoided even for exact positioning of the foil and laser beam. However, most of the vanadium is dissolved in the weld metal in form of the Al_{10}V phase, resulting in an increased etching behaviour. The addition of vanadium to the weld metal as in case of the first approach joints results in slightly smaller and more equiaxed grains in the fusion zone, when compared to the welds of the second approach. Moreover, the micropores in the first approach welds are considerably smaller as the vanadium-rich inclusions. In contrast, the welds of the second approach possess a very homogeneous microstructure in the fusion zone.

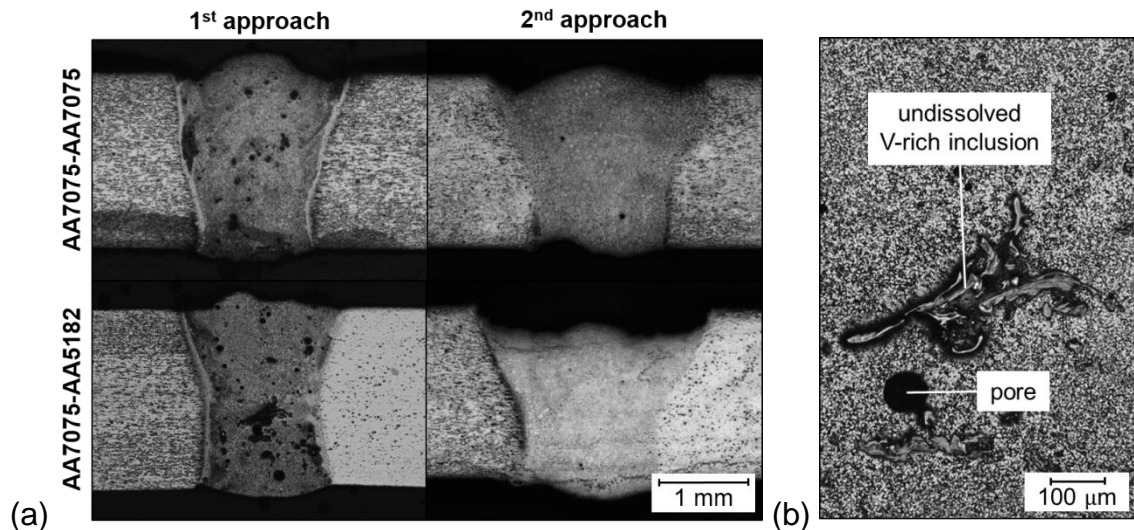


Fig. 4: Macrographs of the similar and dissimilar joints laser beam welded with both approaches (a) and vanadium inclusion in the fusion zone of a first approach joint (b). The porosity in the fusion zone of the vanadium foil welds was caused by the addition of vanadium. It can be assumed that the small size of the pores was induced by hydrogen. The results of the determination of the hydrogen content in Fig. 5 confirm this assumption. The similar welds of the first approach exhibit more than three times higher hydrogen content as the second approach weld and the base material AA7075. Furthermore, the scatter of the results is very large for the vanadium foil approach. However, the oxide on the surface of the thin vanadium foil could hardly be removed without destroying the foil. The very low hydrogen content of the second approach can be explained by the use of the fiber laser with a large beam diameter, which enabled a good degassing during laser beam welding.

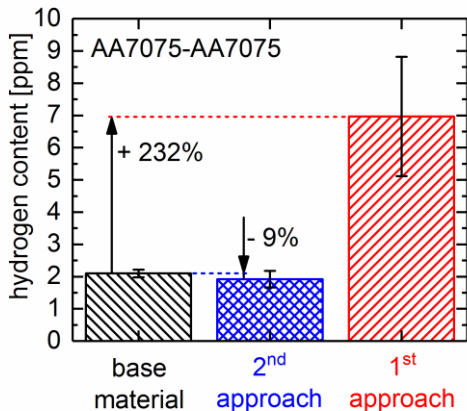


Fig. 5: Hydrogen content of the base material and the similar AA7075-AA7075 joints welded with both approaches (each average of three measurements). More details on the thermophysical fundamentals of the developed approaches and their effect on the weldability can be found in the previous studies of the authors [21,22]

3.2. Mechanical properties

In Fig. 6 the microhardness profiles for both joint configurations and approaches are depicted. It can be seen that the hardness in the fusion zone of the first approach joint is higher as for the second approach joint. This can be explained by the presence of vanadium, which exhibits a high initial hardness of approximately 630 HV. Furthermore, it becomes obvious that the precipitation-hardenable Al-Zn-Mg-Cu alloy 7075 was affected by the heat in the vicinity of the fusion zone, the so-called heat affected zone (HAZ). The naturally aged Al-Mg alloy 5182 did not show any degradation of hardness. The microhardness of the fusion zone and the heat affected zone was always lower as the AA7075 base material.

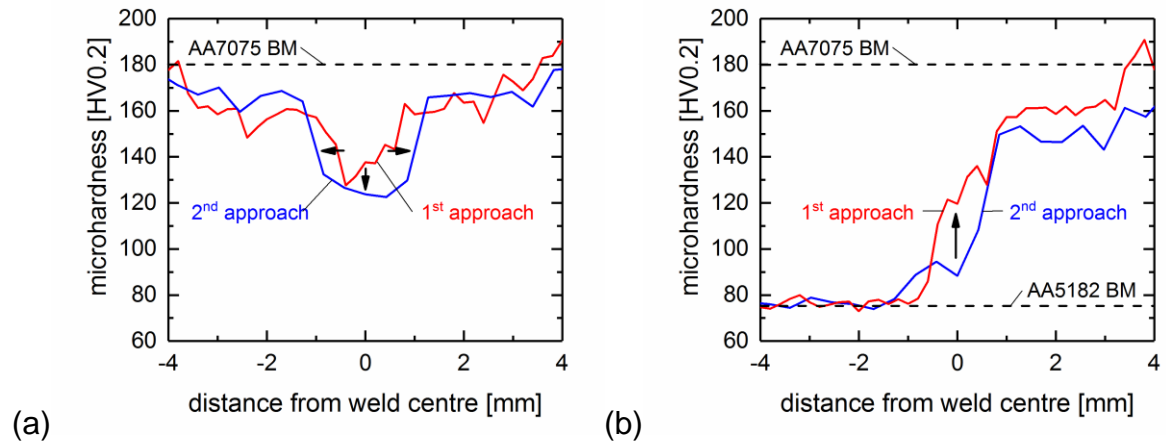


Fig. 6: Microhardness profiles of the similar (a) and dissimilar (b) joint for both approaches.

Post-weld heat treatment is an appropriate method for reducing the hardness loss in the fusion and heat affected zone. However, often this method is not applicable or cost-efficient, in particular for large structures. The effect of the post-weld heat treatment on the welded joints of both joint configurations and approaches is depicted in Fig. 7. Although the fusion zone of the first approach possess a higher initial hardness, it was not possible to raise the microhardness to the level of the base material. In case of the second approach, post-weld heat treatment enabled the elimination of the hardness drop in the heat affected zone of the welds. Because Al-Mg alloys are not precipitation-hardenable, no effect of the post-weld heat treatment was observed for the AA5182 base material and only an almost negligible effect on the fusion zone, which represents a chemical mixture of the aluminum alloys 5182 and 7075.

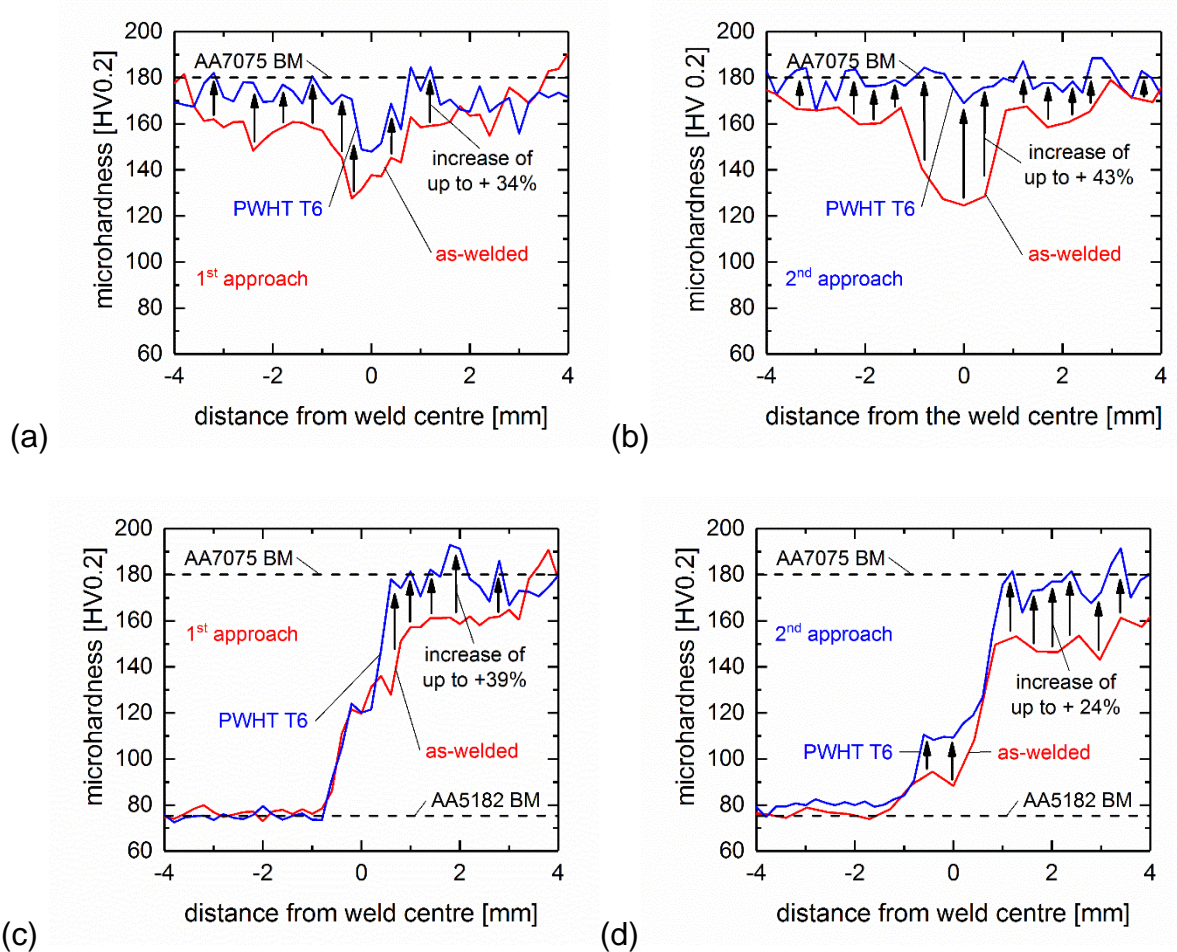


Fig. 7: Effect of post-weld heat treatment to T6 on the microhardness of the similar joints (a)+(b) and dissimilar joints (c)+(d) of both approaches.

Figure 8 shows the stress-strain curves of the welded joints of both approaches in comparison to the base materials. The results of the tensile tests are summarized in Table 3. The precipitation-hardenable Al-Zn-Mg-Cu alloy 7075 exhibits almost twice of the ultimate tensile strength as the naturally aged Al-Mg alloy 5182. Due to welding, a considerable loss of strength and ductility was observed for both aluminum alloy combinations. The reason for this lies in the fact that strain constraint in the weak fusion zone occurred [14]. For fusion welding techniques joint efficiencies for the ultimate tensile strength of 50% to 80% of the base material level and for the elongation of 10% to 30% are typical for precipitation-hardenable aluminum alloys [15,16]. In case of friction stir welding slightly higher values can be achieved

[16,17,18]. The inferior tensile properties of the first approach, in spite of the high microhardness, can be explained by the presence of vanadium-rich inclusions, which represent a metallurgical inhomogeneity causing crack initiation. This leads to an earlier failure during tensile testing. In case of the dissimilar joint a higher ductility was obtained, since the Al-Mg alloy exhibits a lower strength as the weld zone. The serrated flow typical for the Portevin-Le Chatelier effect indicates that the deformation occurred predominantly in the AA5182 sheet [23]. However, due to geometrical discontinuities the failure still occurred along the fusion zone.

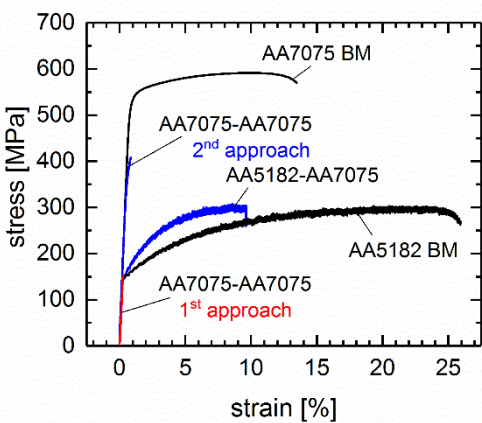


Fig. 8: Stress-strain curves of the base materials and joint configurations laser beam welded with both approaches in the as welded condition.

Table 3: Tensile properties of the base materials and joint configurations laser beam welded with both approaches in the as welded and milled condition in brackets.

material / joint configuration	YS [MPa]	UTS [MPa]	e _f [%]
AA5182-O BM	149.8	303.5	25.6
AA7075-T6 BM	525.3	592.1	13.4
AA7075-AA7075 - 1 st approach	n.a.	151.7 (118.4)	0.2 (0.2)
AA7075-AA7075 - 2 nd approach	n.a.	358.2 (408.3)	0.21 (0.26)
AA5182-AA7075 - 2 nd approach	148.9 (161.2)	260.3 (307.1)	2.9 (9.3)

The milling of the surface had a large effect on the resulting tensile properties and joint efficiencies, as it can be seen in Fig. 9. Therefore, the effect of surface notches, which can lead to stress concentration, was eliminated by the improvement of the surface condition. In case of the dissimilar joint of the second approach a ductility increase of more than 300% was observed. Thus, it can be stated that the weld zone can be protected from damage under quasi-static tensile load by the mechanical mismatch of both aluminum alloys, in terms of strength and ductility. However, the negative effect of the vanadium-rich inclusions could not be compensated by surface milling. As a result, all determined values of the first approach show a large scatter. Although a measurable effect for surface milling could be achieved in case of the second approach, it is often not applicable for large structures mainly due to the high manufacturing effort.

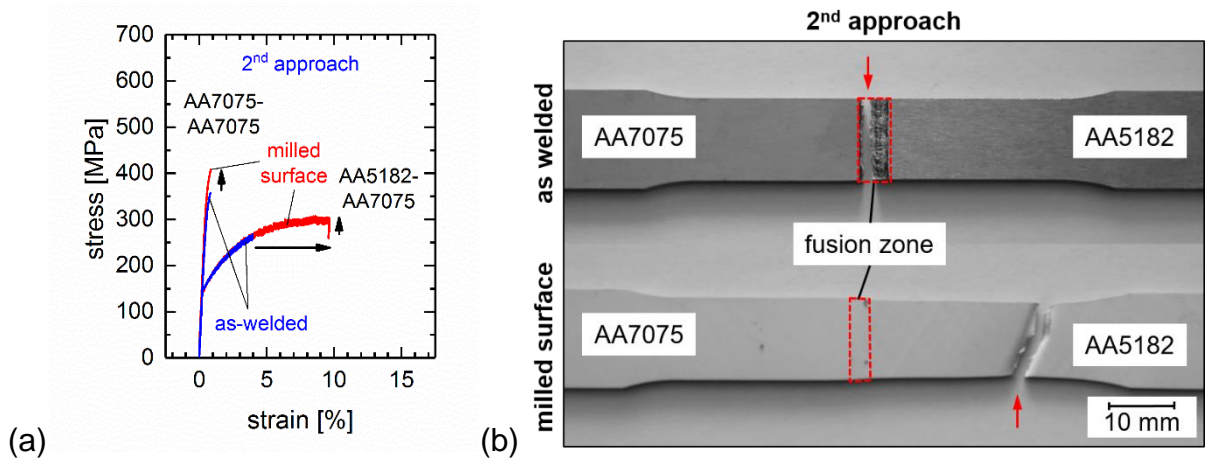


Fig. 9: Effect of the surface condition on the tensile properties (a) and the location of failure (indicated by a red arrow) (b) for the second approach joints.

The results for the limit dome height testing of the base materials are depicted in Fig. 10. It can be seen that for forming at 230°C the required load was reduced to almost the half. Moreover, a slight ductility increase could be observed. The improved formability at elevated temperature resulted from the static recovery of material,

which is generally characterized by a reduced dislocation density and polygonisation [24,25].

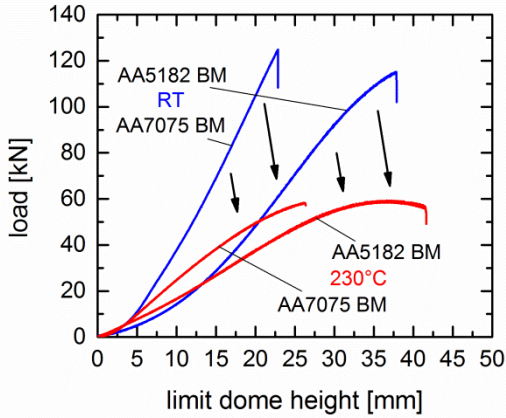


Fig. 10: Load displacement curves of the base materials at two different forming temperatures.

Fig. 11 shows the results for the limit dome height testing of welded joints. Similar to the results of the tensile tests, the formability of the welded joints is inferior in direct comparison to the base materials (Fig. 10). The lowest formability was observed for the first approach joints. The presence of metallurgical inhomogeneities, the vanadium-rich inclusions, resulted in the early failure of the joints. Even in case of forming at elevated temperature, no improvement of formability was achieved. The joints of the second approach possess a slightly better formability. For both approaches, the dissimilar joint configurations exhibit the highest formability, due the use of the more ductile Al-Mg alloy 5182. In this case, a limit dome height of up to 55% of the high-strength AA7075 base material and 33% of the ductile AA5182 base material were obtained. Forming of the base materials at elevated temperature led to a reduction of the required punch load (Fig. 10). However, no considerable improvement of formability was observed for the welded joints in comparison to the base materials. The reason for this is again the strain constraint within the softer fusion zone. The apparently converse forming behavior of the first approach joints

can be explained by the deviation of the results due to the metallurgical inhomogeneities in the fusion zone. The similar joints of the second approach showed no abrupt failure with a considerable reduction of the punch load but a failure initiation and propagation with a lower increase of the punch load. This means that the crack propagation was temporary impeded within the fusion zone. The abrupt failure of the other welds can be explained by metallurgical inhomogeneities and large strength mismatch leading to strain constraint. The results of the limit dome height testing are also summarized in Table 4.

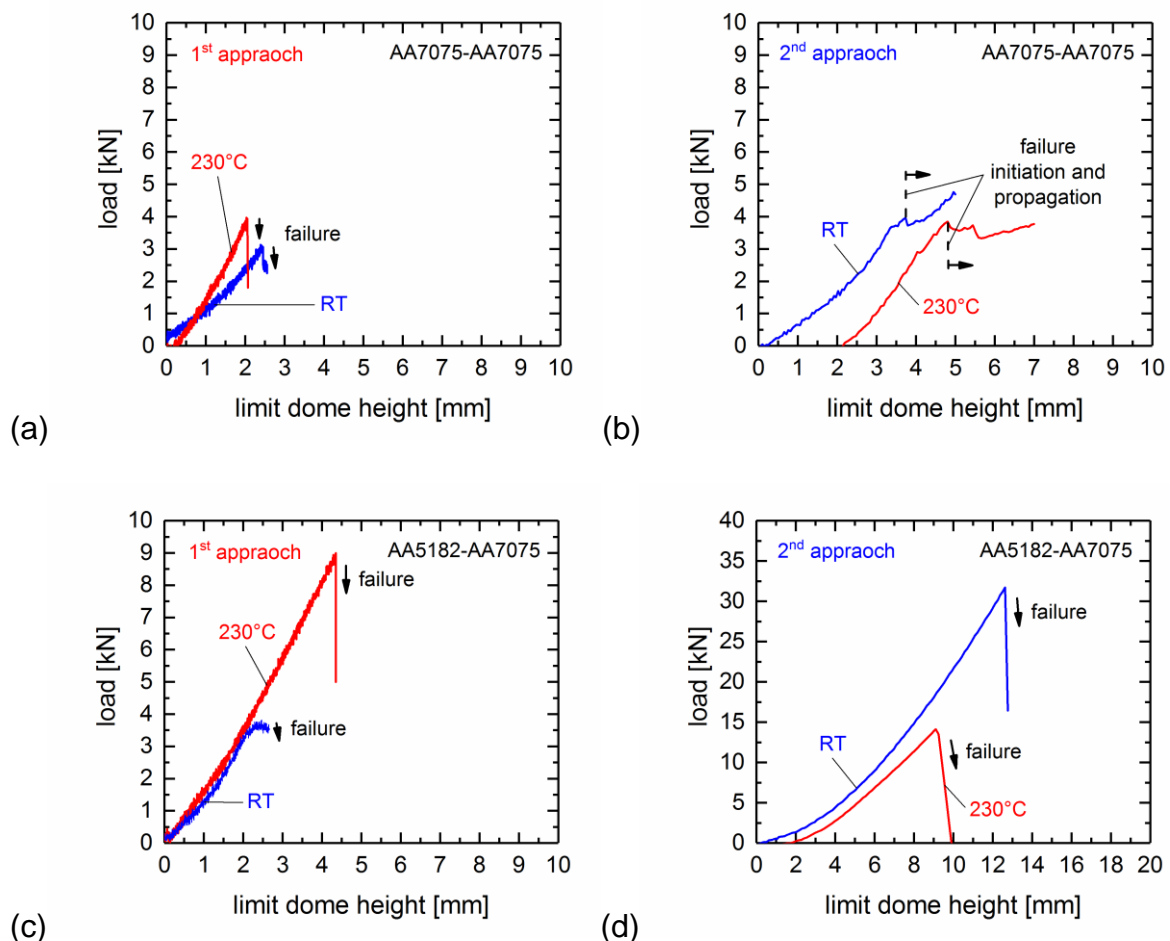


Fig. 11: Load displacement curves of the similar joints (a)+(b) and dissimilar joints (c)+(d) of both approaches.

The differences in appearance of the dome samples are shown in Fig.12. The material with the highest formability, AA5182, formed an almost hemispherical dome

shape. In contrast, the welded joints formed very flat dome. The location of failure during limit dome height testing differed for the base materials. In case of the welded similar and dissimilar joints, the failure always occurred along the softer fusion zone and perpendicular to the rolling direction of the sheets. Because the joints were LDH tested in the as-welded condition, the protective effect of the ductile Al-Mg sheet on the weld zone, observed for milled tensile specimens, is limited.

Table 4: Measured limit dome height (in mm) for the hemispherical dome stretch test of the investigated base materials and joint configurations laser beam welded with both approaches.

material / joint configuration	at RT	at 230°C
AA5182-O BM	37.8	41.5
AA7075-T6 BM	22.6	26.3
AA7075-AA5182 - 1 st approach	2.7	4.3
AA7075-AA7075 - 1 st approach	2.5	2.1
AA7075-AA5182 - 2 nd approach	12.6	9.2
AA7075-AA7075 - 2 nd approach	3.7	4.8

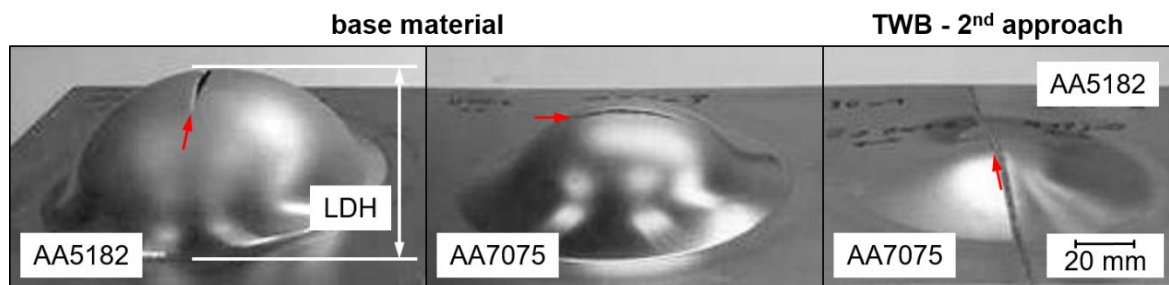


Fig. 12: Photographs of the resulting deformed dome sample of the base materials and a welded joint at 230°C and the location of failure (indicated by a red arrow).

The above-mentioned strain constraint within the fusion zone, resulting in failure initiation, can be seen in the major strain distribution of the first approach joints in Fig. 13. A similar behavior was observed for the second approach joints. As expected,

strain peaks were observed in the softer fusion zone, where deformation localizes. At elevated temperatures, higher strains were achieved, in particular in the heat affected zone of the joints. In case of the dissimilar joints, higher strain for the AA5182 side and a strain peak in the vicinity of the fusion zone on the AA5182 side was observed. The reason for this is the heterogeneity of the mechanical properties of both base materials (the high-strength AA7075 and the more ductile AA5182) and the fusion zone, as a chemical mixture of both base materials and the two filler materials (the AA5087 filler wire and the vanadium foil) [26,27]. The obtained results resemble earlier results for laser beam welded similar AA5182-AA5182 joints [12,14].

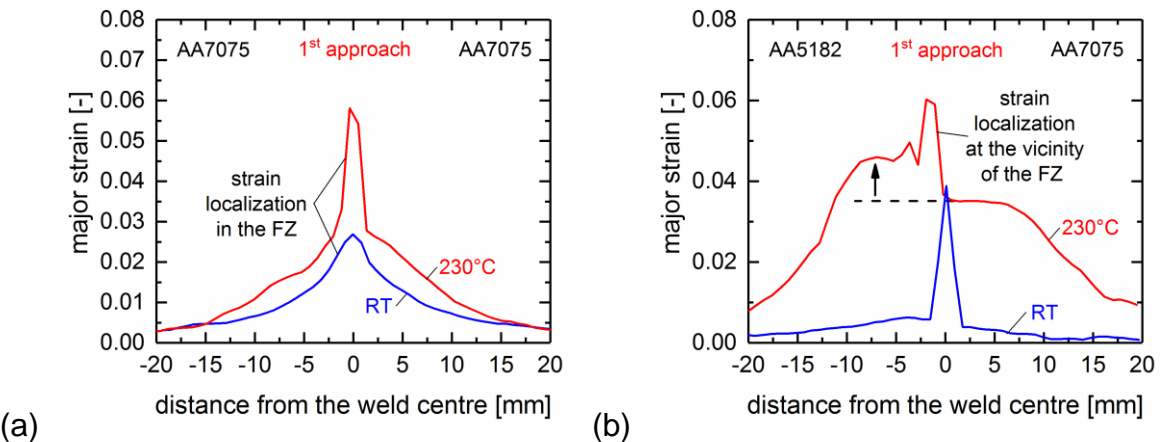


Fig. 13: Exemplary major strain distribution across the joints of the first approach.

4. Conclusions

On the basis of the obtained findings of the study the following conclusions can be drawn:

- (1) Laser weldability of similar and dissimilar joints with an Al-Zn-Mg-Cu alloy was achieved by the use of the two developed approaches, implying either the use of a vanadium foil as additional filler material or the use of a fiber laser with a large beam diameter. Weld discontinuities were reduced to a minimum. Moreover, the outer appearance of the welds was improved.

- (2) The welds of both approaches exhibit different chemical and microstructural features, which finally result in different mechanical properties. Due to the addition of vanadium foil for the first approach, the fusion zone shows vanadium-rich inclusions, a vanadium containing phase as well as slightly smaller and more equiaxed grains.
- (3) Although the addition of vanadium for the first approach led to a local increase of microhardness, the resulting tensile and forming properties are inferior in comparison to the fiber laser joints of the second approach due to their character as metallurgical inhomogeneity.
- (4) The dissimilar joints represent a mechanical mismatch configuration due to the differing mechanical properties of the Al-Zn-Mg-Cu and Al-Mg alloy sheets. Thus, the weld zone could be protected from damage under quasi-static tensile load and partly during the forming process by the more ductile Al-Mg alloy.
- (5) Different strategies for improving the resulting mechanical properties of welded precipitation-hardenable aluminum alloys were proposed, such as post-weld heat treatment, surface milling and warm forming. However, their applicability for large-scale structures is very limited. For this reason, laser welded aluminum TWB's (in the as-welded condition) are only applicable for structures with a relatively low forming degree.

References

- [1] Mondolfo, L. F. 1976. Aluminium Alloys – Structure and Properties. Butterworths, London.
- [2] Allen, C.M., Verhaeghe, G., Hilton, P.A., Heason, C.P., Prangnell, P.B., 2006. Laser and hybrid laser-MIG welding of 6.35 and 12.7 mm thick aluminium

aerospace alloy. Materials Science Forum, 519, pp. 1139-1144.

<http://dx.doi.org/10.4028/www.scientific.net/MSF.519-521.1139>

- [3] Verhaeghe, G. 2008. Achieving aerospace standard porosity levels when welding thin and thick-section aluminium using fibre-delivered lasers. Dissertation, University of Warwick.
- [4] Mahoney, M.W., Rhodes, C.G., Flintoff, J.G., Bingel, W.H., Spurling, R.A. 1998. Properties of friction-stir-welded 7075 T651 aluminium. Metallurgical and Materials Transactions A, 29(7), pp. 1955-1964.
<http://dx.doi.org/10.1007/s11661-998-0021-5>
- [5] Smith, C.B., Crusan, W., Hootman, J.R., Hinrichs, J.F., Heideman, R.J., Noruk, H.J.S. 2001. Friction stir welding in the automotive industry. Proceedings of the TMS 2001, New Orleans, pp.175-185.
- [6] Threadgill, P.L., Leonard, A.J., Shercliff, H.R., Withers P.J. 2009. Friction stir welding of aluminium alloys. International Materials Reviews, 54(2), pp. 49-93.
<http://dx.doi.org/10.1179/174328009X411136>
- [7] Fridlyander, I. N., Sister, V. G., Grushko, O. E., Berstenev, V. V., Sheveleva, L. M., Ivanova, L. A. 2002. Aluminum alloys: promising materials in the automotive industry. Metal Science and Heat Treatment, 44(9-10), pp. 365-370. <http://dx.doi.org/10.1023/A:1021901715578>
- [8] van Nieuwerburgh, D. 2011. Aluminium sheet developments for current and future BIW concepts. In: Aluminium Experience Day, Aleris Europe.
- [9] Friedman, P.A., Kridli, G.T. 2000. Microstructural and mechanical investigation of aluminium tailor-welded blanks. Journal of Materials Engineering and Performance, 9(5), pp. 541-551.
<http://dx.doi.org/10.1361/105994900770345674>

- [10] Davies, R. Oliver, H.E., Smith, M.T., Grant, G.J. 1999. Characterizing Al tailor-welded blanks for automotive applications. JOM, 51(11), pp. 46-50.
<http://dx.doi.org/10.1007/s11837-999-0222-4>
- [11] Davies, R.W., Smith, M.T., Oliver, H.E., Khaleel, M.A., Pitman, S.G. 2000. Weld metal ductility in aluminium tailor welded blanks. Metallurgical and Materials Transactions A 31(11), pp. 2755-2763.
<http://dx.doi.org/10.1007/BF02830335>
- [12] Kinsey, B., Viswanathan, V., Cao, J. 2001. Forming of aluminium tailor welded Blanks. SAE Technical Paper, No. 2001-01-0822, pp. 91-97.
<http://dx.doi.org/10.4271/2001-01-0822>
- [13] Kridli, G., Friedman, P.A., Sherman, A.M. 2000. Formability of aluminium tailor-welded blanks. SAE Technical Paper. No. 2000-01-0772, pp. 57-65.
<http://dx.doi.org/10.4271/2000-01-0772>
- [14] Ahn, J., Chen, L., He, E., Davies, C. M., Dear, J. P., 2017. Effect of filler metal feed rate and composition on microstructure and mechanical properties of fibre laser welded AA 2024-T3. Journal of Manufacturing Processes, 25, pp. 26-36.
<https://dx.doi.org/10.1016/j.jmapro.2016.10.006>
- [15] Stasik, M.C., Wagoner, R.H. 1996. Forming of tailor-welded aluminium blanks. Minerals, Metals and Materials Society, pp. 69-83.
- [16] Vilaça, P, Santos, J.P, Góis, A, Quintino, L. 2005. Joining aluminium alloys dissimilar in thickness by friction stir welding and fusion welding processes. Welding in the world, 49(3-4), pp. 56-62.
<http://dx.doi.org/10.1007/BF03266476>
- [17] Zadpoor, A.A., Sinke, J., Benedictus, R., Pieters, R. 2008. Mechanical properties and microstructure of friction stir welded tailor-made blanks.

Materials Science and Engineering: A, 494(1), pp. 281-290.

<http://dx.doi.org/10.1016/j.msea.2008.04.042>

- [18] Kesharwani, R. K., Basak, S., Panda, S. K., Pal, S. K., 2017. Improvement in limiting drawing ration of aluminum tailored friction stir welded blanks using modified conical tractrix die. Journal of Manufacturing Processes, 28, pp. 137-155.

<https://dx.doi.org/10.1016/j.jmapro.2017.06.002>

- [19] Wu, S.C., Yu, X., Zuo, R. Z., Zhang, W. H., Xie, H. L., Jiang, J. Z., 2013. Porosity, element loss, and strength model on softening behavior of hybrid laser arc welded Al-Zn-Mg-Cu alloy with synchrotron radiation analysis. Welding Journal, 92(3), pp. 64-71.

- [20] Jiang, Y. S., Yang, S. L., Wang, Y., Yang, Z. H., 2017. Research on the microstructure and mechanical properties of fiber laser welding of A7N01 Al-alloy. In: Key Engineering Materials, Trans Tech Publication. 734. Pp. 310-318.

<http://dx.doi.org/10.4028/www.scientific.net/KEM.734.310>

- [21] Enz, J., Riekehr, S., Ventzke, V., Huber, N., Kashaev, N., 2016. Laser weldability of high-strength Al-Zn alloys and its improvement by the use of an appropriate filler material. Metallurgical and Materials Transactions A, 47(6), pp. 2830-2841. <http://dx.doi.org/10.1007/s11661-016-3446-2>

- [22] Enz, J., Riekehr, S., Ventzke, V., Huber, N., Kashaev, N., 2016. Fibre laser welding of high-alloyed Al-Zn-M-Cu alloys. Journal of Materials Processing Technology, 237, pp. 155-162.

<http://dx.doi.org/10.1016/j.jmatprotec.2016.06.002>

- [23] Romhanji, E., Glisic, D., Milenkovic, V., 2001. Forming aspects of high-strength Al-Mg alloy sheet. *Materiali in Tehnologije*, 35(1/2), pp. 21-26.

- [24] Gundlach, C., 2006. Recovery in aluminium. Doctoral dissertation, Technical University of Denmark (DTU).
- [25] Kumar, M., Sotirov, N., Chimani, C. M. 2014. Investigations on warm forming of AW-7020-T6 alloy sheet. *Journal of Materials Processing Technology*, 214(8), pp. 1769-1776. <http://dx.doi.org/10.1016/j.jmatprotec.2014.03.024>
- [26] Leitão, C., Emílio, B., Chaparro, B.M., Rodrigues, D.M., 2009. Formability of similar and dissimilar friction stir welded AA 5182-H111 and AA 6016-T4 tailored blanks. *Materials and Design*, 30, pp. 3235-3242.
<http://dx.doi.org/10.1016/j.matdes.2008.12.005>
- [27] Bhagwan, A.V., Kridli, G.T., Friedman, P.A. 2004. Formability improvement in aluminium tailor-welded blanks via material combinations. *Journal of Manufacturing Processes*, 6(2), pp. 134-140. [http://dx.doi.org/10.1016/S1526-6125\(04\)70067-5](http://dx.doi.org/10.1016/S1526-6125(04)70067-5)

Biographies

Josephin Enz completed her studies in Mechanical Engineering with specialisation in Materials Engineering at the Hamburg University of Technology in 2012. Accompanying to her studies she graduated as an International Welding Engineer in 2009. In 2016 she completed her Ph.D. studies at the Hamburg University of Technology (pending certificate). Since 2016 she also became junior group leader of the CALMS group (Characterisation of Laser Additive Manufactured Structures) at the department Joining and Assessment at the Helmholtz Zentrum Geesthacht.

Dr. Manoj Kumar studied processing of aluminium alloys at Vienna University of technology, Austria and proceeded to work in Austrian institute of technology. He worked in development of new aluminium alloys and their casting and forming technologies and published over 20 articles in peer-reviewed conferences and journals. Currently he is working to develop an innovative, intelligent and cost-effective heat process technology for aluminium alloys in EBNER Industrieofenbau GmbH, Austria.

Stefan Riekehr concluded his studies in Materials Sciences at the Clausthal University of Technology as a graduate engineer in 1995. Since 1996, he has worked at the Helmholtz Centre in Geesthacht, "Joining and Assessment" Department and is responsible for materials testing and the fracture-mechanical assessment of laser-welded joints. Moreover, he has been responsible for laser welding activities since 2001.

Dr. Volker Venzke acquired his Ph.D. degree in Materials Science from the Clausthal University of Technology in 2014. Since 1996, he has worked as a scientist at the Helmholtz Centre in Geesthacht (formerly the Research Centre of the Society for Nuclear Energy Utilisation in Shipbuilding and Shipping - GKSS), "Joining and

Assessment" Department and is responsible for their materials analytics laboratory (SEM, EDX, EBSD, gas analytics and metallography).

Prof. Dr. Norbert Huber obtained his PhD degree in Mechanical Engineering in 1996 from University of Karlsruhe. In 2001 he became head of Department "Materials Mechanics 1" at the Forschungszentrum Karlsruhe, Institute of Materials Research II. In 2006 he accepted an offer for a position as Professor for Materials modelling and Simulation from Hamburg University of Technology and became at the same time head of Institute of Materials Research at Helmholtz-Zentrum Geesthacht, a member of the Helmholtz-Association. Since 2009 Prof. Huber is speaker of the Helmholtz Programme "Advanced Engineering Materials".

Dr. Nikolai Kashaev concluded his studies in Energy-Related Mechanical Engineering with the advanced subject of electrical aerospace engines and power plants at the Bauman University of Technology in Moscow in 2001. Subsequently, he worked as a scientific employee at the Foundation Institute for Materials Technology in Bremen for four years. In 2005, he obtained his doctoral degree in Materials Science. After various activities in industry, he has been the head of the "Joining and Assessment" Department at the Institute for Materials Research and Materials Mechanics at the Helmholtz Centre in Geesthacht since 2010.